



Electron Beam Bonding: a novel method for joining additively manufactured carbon fiber thermoplastic composites with aluminum to produce multi-material joints for lightweight applications

Aybike Yalçınyüz¹ · Julius Raute¹ · Joamin Gonzalez-Gutierrez² · Eujin Pei³ · Max Biegler¹ · Michael Rethmeier^{1,4,5}

Received: 22 February 2025 / Accepted: 2 June 2025 / Published online: 24 June 2025
© The Author(s) 2025

Abstract

In recent years, new solutions have been explored to reduce the weight of components for the automotive, railway, and aerospace industries. For this reason, Carbon Fiber Composites (CFCs) have increasingly replaced metals in products that need to be lightweight. However, due to their poor thermal conductivity, CFCs have limited use in applications requiring efficient heat dissipation. In such applications, conventionally manufactured metal alloys are typically utilized. To address these limitations, a novel approach using a combination of additively manufactured aluminum and CFCs is proposed to exploit the distinct advantages of both materials. These innovative hybrid structures aim to combine good structural and thermal management properties with reduced weight compared to conventionally produced metal products. In this study, additively manufactured aluminum alloy (AlSi10Mg) and short carbon fiber Polyamide 6 composite (sCF-PA6) are utilized to produce metal–polymer pairs using electron beam energy to bond the two materials. Direct irradiation of short CFCs with electron beam leads to polymer degradation. Thus, a novel method “Electron Beam Bonding” for joining CFCs with aluminum alloy in various joint configurations using electron beam technology is demonstrated. This innovative approach presents a promising solution for creating metal–polymer multi-materials for lightweight applications.

Keywords Electron beam bonding · Multi-material · Lightweight · Additive manufactured materials · Short carbon fiber composites · AlSi10Mg · Joining

✉ Aybike Yalçınyüz
aybike.yalcinyuez@ipk.fraunhofer.de

✉ Joamin Gonzalez-Gutierrez
joamin.gonzalez-gutierrez@list.lu

✉ Eujin Pei
eujin.pei@brunel.ac.uk

Julius Raute
maximilian.julius.raute@ipk.fraunhofer.de

Max Biegler
max.biegler@ipk.fraunhofer.de

Michael Rethmeier
michael.rethmeier@ipk.fraunhofer.de

¹ Fraunhofer Institute of Production Systems and Design Engineering (IPK), Berlin, Germany

² Luxembourg Institute of Science and Technology (LIST), Hautcharage, Luxembourg

³ Brunel University of London, Uxbridge, United Kingdom

⁴ Technische Universität Berlin, Berlin, Germany

⁵ Federal Institute For Materials Research and Testing, Berlin, Germany

1 Introduction

Electrical and electronic equipment must efficiently dissipate accumulated heat to protect sensitive components. Traditionally, this is achieved using metal alloys [1]. Today, the lightweight potential, low cost, and acceptable thermo-mechanical properties of carbon fiber-reinforced polymer composites make them excellent candidates to replace metals [2, 3]. Currently, CFCs are primarily used for structural applications because of poor thermal conductivity. To address this, multi-material structures combining aluminum and CFCs are proposed for lightweight products with integrated thermal management.

Achieving a strong bond between dissimilar materials is challenging due to differences in their physical and chemical properties, particularly the significant variations in their melting temperatures and thermal conductivities. In recent years, the joining of metals and polymer materials has been researched due to the intense demand for lightweight structures. The most used joining technologies for polymer–metal

hybrid structures in the literature are adhesive bonding, mechanical fastening, mechanical joining, solid-state welding, and combinations of these technologies, such as friction stir welding [4], mechanical clinching [5], self-piercing riveting [6], and ultrasonic plastic welding [7]. Although these processes offer advantages such as being cost-effective, environmentally friendly, and easily accessible, there are limitations regarding joint types, thickness, geometry, and surface quality. Defects, such as delamination, cracks, bubbles, and poor adhesion, can also occur on the composite parts [8]. Electron Beam Welding (EBW) addresses these shortcomings by enabling welding in a vacuum chamber to prevent oxidation and joining of materials with different melting temperatures [9]. EBW is versatile, accommodating various shapes and joint types, such as lap, butt, T-, and corner joints [10].

This study presents electron beam technology for joining dissimilar materials through a process called Electron Beam Bonding. The process capabilities are demonstrated by bonding Additively Manufactured (AM) short carbon fiber (sCF) reinforced Polyamide 6 (PA6) specimens with AlSi10Mg aluminum alloy specimens.

2 Materials and methods

A PA6 composite PolyMide™ PA6-CF [Polymaker, China] in 1.75 mm filaments was used for bonding specimens manufactured via Material Extrusion with a NeoCore303 machine [D33D, France]. AlSi10Mg specimens were produced using a Print Sharp 150 Laser Powder Bed Fusion (LPBF) machine [Prima Additive S.r.l., Italy] with gas-atomised powder [m4p material solutions GmbH, Germany]. The joining process was done using an EBG15-150 K30 electron beam welding system [pro-beam GmbH, Germany] at a constant acceleration voltage of 120 kV, with pressure ranging from 3×10^{-4} to 4×10^{-4} mbar. Specimens were manually clamped by hand until they could no longer move, and the clamping force was not measured. Sample temperature was measured with 0.2 mm K-type thermocouples connected a

QuantumX MX1609KB module and data analysis was performed using the Catman software [Hottinger Brüel&Kjær GmbH, Germany].

The samples of sCF-PA6 were analyzed after the electron beam application using a light microscope. The thermal conductivity of sCF-PA6 and AlSi10Mg was measured with a Quickline-50 thermal interface analyser [Anter Co., USA]. Lap shear tests, following ASTM D5868-01–202, were conducted at room temperature with a loading rate of 13 mm/min to assess the bond strength and durability. Test coupons measured 175 mm × 25, 4 mm × 6 mm, with a 25 mm overlap, using a ZwickRoell Z150 testing machine [ZwickRoell GmbH & Co. KG, Germany] with a 150 kN load cell.

3 Results

3.1 Development of electron beam bonding

The first step involved assessing the electrical conductivity of CFCs for stable electron emission. sCF-PA6 composites due to their carbon fiber content are suitable for this method [9]. Pre-experiments were conducted to evaluate the thermal behavior of 1 mm-thick sCF-PA6 samples along a 40 mm weld line under various parameters (see Table 1). The spot size of the beam was realized using a standardized beam figure of concentric circles, which was deflected at a frequency of 1000 Hz to achieve the desired magnitude.

Despite using significantly lower energy per unit length compared to 30 J/mm–40 J/mm required to penetrate 1 mm-thick aluminum, sCF-PA6 tends to evaporate during the process (Fig. 1 E02 and E04). sCF-PA6's thermal conductivity is very low (0.34 ± 0.04 W/m K) compared to AlSi10Mg (127 ± 10 W/m K), causing heat to concentrate at the beam impact point, leading to melting and evaporation. When the electron beam size is increased, energy is further distributed across the surface, leading to variations in the size of the resulting “V” shape (Fig. 1 E06), and evaporation was the worst when the energy was further increased (Fig. 1 E08).

Table 1 Process parameters of preliminary experiments

Experiment no	Beam current (mA)	Process speed (mm/s)	Energy per unit length (EpUL) (J/mm)	Spot diameter (mm)
E01	0.1	30	0.4	1
E02	0.1	15	0.8	1
E03	0.1	30	0.4	2
E04	0.1	15	0.8	2
E05	0.1	30	0.4	2.5
E06	0.1	15	0.8	2.5
E07	0.2	30	0.8	2.5
E08	0.2	15	1.6	2.5

Short carbon fiber composites are unsuitable for direct electron beam processing due to low thermal conductivity and thermal stability (Fig. 1). To bond these composites with metals “Electron Beam Bonding” is proposed, which involves controlled heating of the metal part to the composite’s softening temperature through direct contact, causing localized melting and adhesion. A similar approach has been reported using laser beams [11–14]. Electron Beam Bonding is illustrated in Fig. 2.

Feasibility studies were conducted on both joint types using sCF-PA6 and AlSi10Mg plates, each 3 mm thick. In these studies, AlSi10Mg samples were heated to temperatures of 280 °C or higher, using beam currents of either 2 mA or 2.5 mA. It was observed that achieving a measured temperature of 280 °C or more in both setups (i.e., butt and overlap joints) resulted in successful bonding. This is significant, because the material extrusion temperature for sCF-PA6 ranges between 280 °C and 300 °C. Based on the placement of the thermocouples, it is anticipated that the temperature at the interface may exceed 280 °C, but it is likely to remain below the degradation temperature of PA6, which is ~390 °C [15]. If the temperature were to exceed this threshold, degradation could occur, leading to the formation of pores similar to those shown in Fig. 1. The cooling process was much slower than laser processes [16], because it relies solely on conduction, with no convection is available due to the vacuum conditions (Fig. 3). Scanning areas measured 70 mm × 10 mm for butt joints and 35 mm × 25 mm for

overlap joints, with energy applied to 1000 discrete points in these areas. To determine the energy input into the metal part, the energy per unit area (EpUA) was calculated by converting the energy per unit length (EpUL) [9] using Eq. 1. A 1 mm joining distance (Fig. 2, right) was maintained to avoid direct beam interaction with the composite. Results indicate that this method is suitable for joining metal and composite parts (Fig. 3).

$$\text{Energy per unit area} \left[\frac{\text{J}}{\text{mm}^2} \right] = \frac{\text{Beam current [mA]} \times \text{Acceleration voltage [kV]} \times \text{Heating time [s]}}{\text{Scanning area [mm}^2\text{]}} \quad (1)$$

3.2 Bond strength of joints

Ten overlap specimens were produced using a 25 mm overlap length, 2 mA beam current, and a 26 mm × 26 mm scanning area. Lap shear tests were performed, and the results, including peak temperatures, EpUA, lap-shear force, and lap-shear strength, are summarized in Table 2. It is important to note that lap-shear strength was calculated by dividing the force by the overlapping area between the metal and the polymer. The results indicated a consistent lap-shear strength across all ten trials, yielding an average lap-shear strength of 5.4 ± 0.5 MPa, derived from an average maximum lap-shear force of 3.4 ± 0.3 kN.

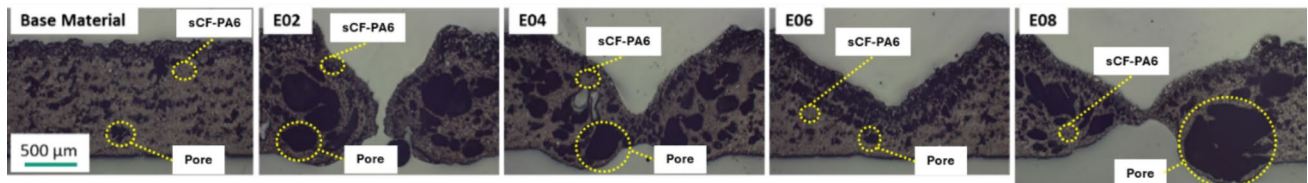


Fig. 1 Cross section of base material (sCF-PA6), experiments with EpUL of 0.8 J/mm (E02, E04, E06) and 1.6 J/mm (E08)

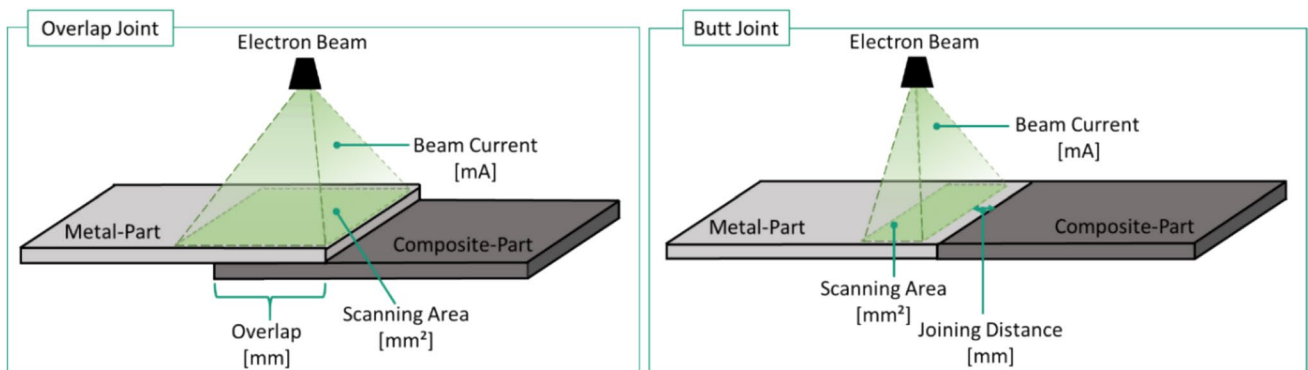


Fig. 2 Method for metal–composite overlap and butt joints using electron beam

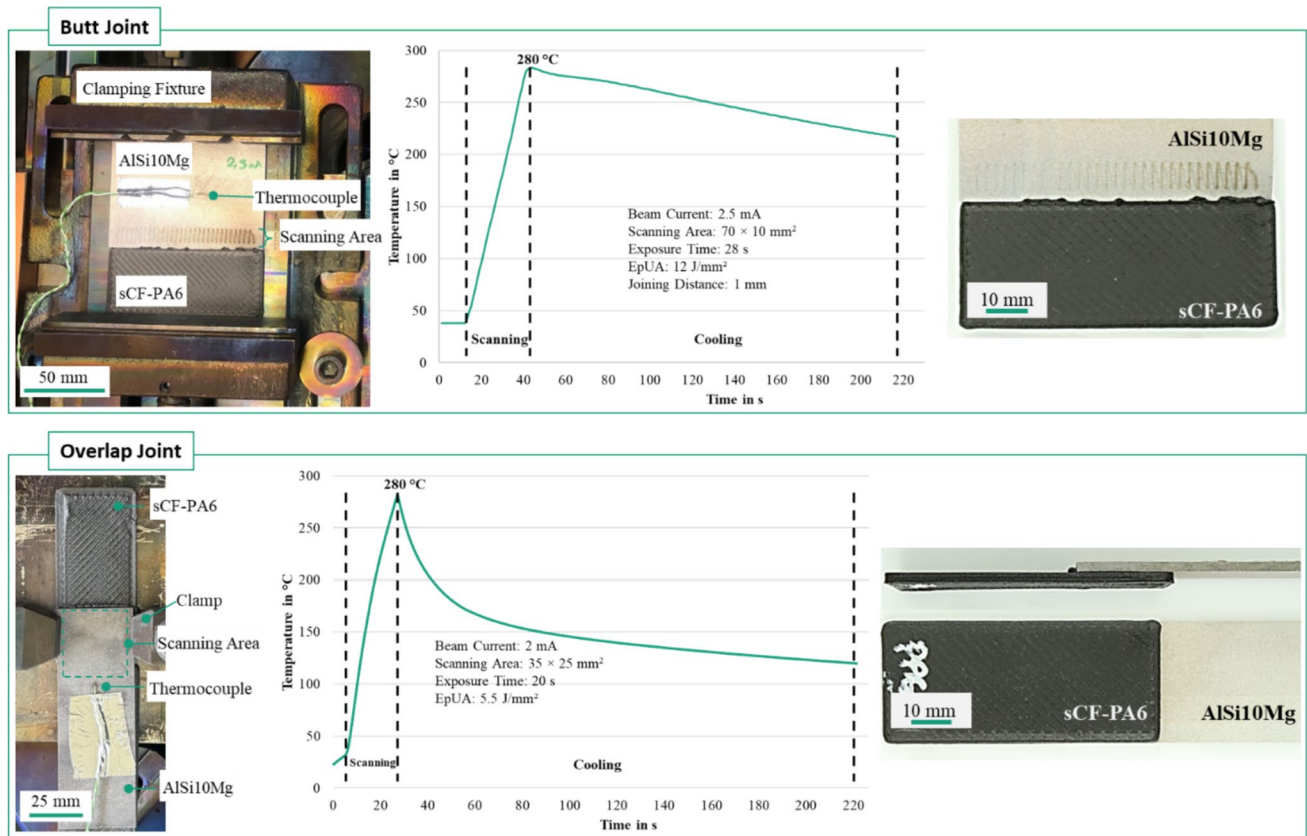


Fig. 3 Experimental setup and temperature measurement during the preparation of butt and overlap joints using electron beam at Fraunhofer IPK, and AlSi10Mg and sCF-PA6 bonded samples

Experiments were conducted at joining temperatures ranging from 280 °C to 290 °C, and no significant differences were observed in lap-shear strength or failure mode. All sCF-PA6 specimens exhibited bulk-substrate failure near the edge of the aluminum specimen. Three specimens (E04, E07, and E08) had strength values below 5 MPa, as indicated by the dotted lines in Fig. 4. The discrepancies in strength

could be attributed to varying clamping forces, as these three specimens appeared more squeezed than others. However, these clamping forces were not measured during the experiments, and we plan to address this in future work.

After the lap-shear tests of the multi-material joints, two types of fracture modes were observed, as shown in Fig. 5.

Table 2 Peak temperature and lap-shear strength of 10 overlap joints

Experiment no	Peak temperature (°C)	Exposure time (s)	EpUA (J/mm^2)	Max. lap-shear force (kN)	Lap shear strength (MPa)
E01	278	16.2	5.8	3.5	5.5
E02	279	17.3	6.1	3.7	5.8
E03	279	17.6	6.2	3.4	5.3
E04	283	17.7	6.3	2.9	4.5
E05	284	16.2	5.8	3.7	5.9
E06	284	17.9	6.4	3.6	5.7
E07	284	17.4	6.2	3.1	4.9
E08	287	17.7	6.3	3.1	4.9
E09	289	17.8	6.3	3.4	5.4
E10	293	17.6	6.2	3.6	5.6

The first type is fracture within the composite material, and the second involves delamination within the composite followed by fracture. These failure modes indicate strong adhesion between the composite and the aluminum, suggesting that the bond strength at the interface exceeds the tensile strength of the composite. As a result, failure occurs within the composite rather than at the joint interface.

4 Discussion

The results show that aluminum-thermoplastic structures can be prepared using electron beam, despite significant differences in thermal properties and mechanical strengths. AlSi10Mg has a thermal conductivity of 127 W/m·K and a melting range between 570 and 590 °C [17], while sCF-PA6 has a thermal conductivity of 0.34 W/m·K and a melting range between 190 and 230 °C as estimated by differential scanning calorimetry, which is in the range reported in the literature [18]. Additionally, the shear strength of AlSi10Mg (~491 MPa) [19] is roughly nine times greater than that of sCF-PA6 (~55 MPa), making strong bonding between these materials challenging.

A review of literature revealed that besides electron beam welding, other methods like Friction Stir Welding (FSW) are commonly used for joining metal and polymer parts. However, FSW often results in joints with inadequate mechanical properties and has limitations related to joint types, geometry, and thickness [4, 20]. These limitations and lower lap-shear strength have led to exploring thermal joining



Fig. 5 Image of fracture patterns of test coupons after the lap-shear test

processes including laser joining [12, 21–23]. Results from this subject are summarized in Table 3.

This study differs from recent laser joining research, because it uses untreated samples. As shown in Table 3, the current results are competitive with findings in the literature, even though they lack surface treatments such as laser texturing that enhance mechanical interlocking [16, 17]. In addition to mechanical interlocking, the EB bonding process involves a physicochemical component that strengthens the bond between sCF-PA6 and AlSi10Mg, similarly to laser methods. For instance, it has been demonstrated that the oxide layer on aluminum positively influences bond strength, as PA6 can form hydrogen bonds with this layer [25]. This

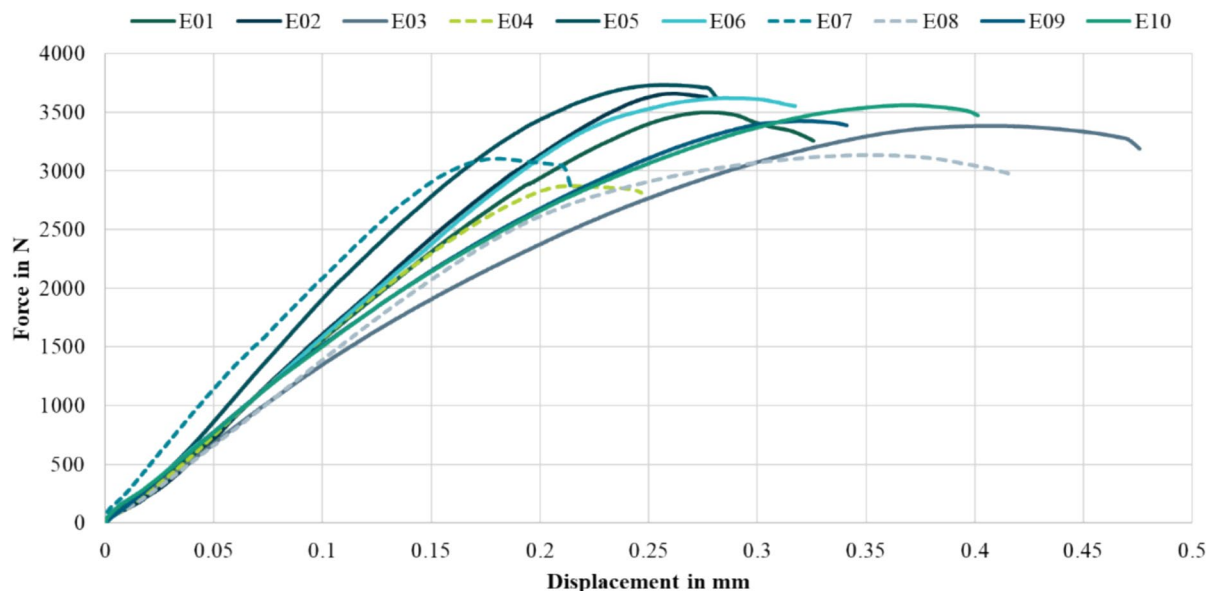


Fig. 4 Graph for load–displacement for experiments E01-E10

Table 3 Literature results on the joining of metal and polymer parts

Reference	Metal part	Polymer part	Joining method	Pre-treatment	Mechanical properties
[4]	AA6082	CF-polyphenylene-sulfide	Friction stir joining	No information	Average lap-shear force: 1920 N
[20]	AA7075	Polyetherether-ketone (PEEK)	Friction-assisted joining	Laser texturing	Average lap-shear force: 5500 N and 5300 N up to surface textured
[12]	AA5052	Long CF-PA6	Laser assisted metal and plastic direct joining	No information	Max. shear force: 3000 N
[21]	AISI 304	Polypropylene or Nylon 66	Laser-based thermo-mechanical joining	Laser texturing	Max. lap-shear force: 750 N for PP and 2200 N for PA66
[22]	Ti6Al4V	Continuous CF -PEEK	Laser joining	Laser texturing	Max. lap joint strength: 58 MPa
[23]	Mild Steel	PA6—glass fiber	Laser joining	Sandblasting or laser texturing	Average lap joint strength: Sand blasted: ca. 8 MPa Surface textured: ca. 29 MPa
[24]	Ti6Al4V	Glass fiber-PEI	Ultrasonic joining	With and without pins	Max. lap-shear force: With pins: 2011 ± 530 N Without pins: 369 ± 29 N
This study	AlSi10Mg	sCF-PA6	Electron Beam Bonding	None	Max. lap-shear force: 3700 N Max. lap joint strength: 5.9 MPa

is another reason why the untreated surface may have contributed to the observed bond strength results.

5 Conclusions

This study demonstrates that the "Electron Beam Bonding" has the potential to effectively bond AM-produced sCF-reinforced thermoplastic composites with aluminum alloys, achieving a maximum lap-shear strength of 5.9 MPa and shear forces of around 3700 N, without surface treatment. Despite its high cost, electron beam technology is an effective tool for developing and testing joining processes for sensitive materials. It allows the precise determination of optimum joining temperatures, heating rates, and strategies. This knowledge can lead to the adoption of simpler, more cost-effective methods, such as hot plates or induction, for industrial series production. Future work will focus on analyzing process parameters and refining the bonding process through surface treatment and clamping techniques to enhance joint strength and reliability, as well as to explore potential industrial use-cases and real-world applications.

Acknowledgements This project was funded by the European Union's Horizon Europe Research & Innovation Programme 2021–2027 under grant agreement number 10109149.

Author contribution The first (1st) and second (2nd) authors collaboratively developed the Electron Beam Bonding method. The first (1st), third (3rd), and fourth (4th) authors worked together within the

EU-Horizon Project and jointly contributed to writing this manuscript. The fifth (5th) and sixth (6th) authors reviewed and provided critical feedback on the manuscript. Note: There is no seventh (7th) author; however, the third affiliation was listed separately to properly attribute Prof. Michael Rethmeier's institutional association.

Funding Open Access funding enabled and organized by Projekt DEAL.

Data availability No datasets were generated or analysed during the current study.

Declarations

Conflict of interest The authors declare no competing interests.

Open Access This article is licensed under a Creative Commons Attribution 4.0 International License, which permits use, sharing, adaptation, distribution and reproduction in any medium or format, as long as you give appropriate credit to the original author(s) and the source, provide a link to the Creative Commons licence, and indicate if changes were made. The images or other third party material in this article are included in the article's Creative Commons licence, unless indicated otherwise in a credit line to the material. If material is not included in the article's Creative Commons licence and your intended use is not permitted by statutory regulation or exceeds the permitted use, you will need to obtain permission directly from the copyright holder. To view a copy of this licence, visit <http://creativecommons.org/licenses/by/4.0/>.

References

1. Zhao C, Li Y, Liu Y, Xie H, Yu W (2023) A critical review of the preparation strategies of thermally conductive and electrically insulating polymeric materials and their applications in

- heat dissipation of electronic devices. *Adv Compos Hybrid Mater* 6(1):27. <https://doi.org/10.1007/s42114-022-00584-2>
2. Mohammadzadeh M, Imeri A, Fidan I, Elkelany M (2019) 3D printed fiber reinforced polymer composites—structural analysis. *Compos B Eng* 175:107112. <https://doi.org/10.1016/j.composb.2019.107112>
 3. Gonzalez-Gutierrez J, Chothe HR, Foyer G, Ten Cate T (2023) Thermoplastic selection for aluminum replacement in electric and electronic devices made by additive manufacturing. Presented at the 1st international conference on lightweight materials. Politecnico di Milano, Milan, Italy, p 107–111
 4. Malaske L, Blaga L-A, Bergmann L, Ahmad B, Zhang X, Klusemann B (2024) Feasibility study of friction stir joining of aluminum with carbon fiber reinforced thermoplastic composite. *J Compos Mater* 58(17):1987–2003. <https://doi.org/10.1177/00219983241254889>
 5. Lambiasi F, Ko D-C (2016) Feasibility of mechanical clinching for joining aluminum AA6082-T6 and carbon fiber reinforced polymer sheets. *Mater Des* 107:341–352. <https://doi.org/10.1016/j.matdes.2016.06.061>
 6. Liu Y, Zhuang W, Luo Y, Xie D, Mu W (2023) Joining mechanism and damage of self-piercing riveted joints in carbon fiber reinforced polymer composites and aluminum alloy. *Thin Walled Struct* 182:110233. <https://doi.org/10.1016/j.tws.2022.110233>
 7. Dal Conte UF, Villegas IF, Tachon J (2019) Ultrasonic plastic welding of CF/PA6 composites to aluminum: process and mechanical performance of welded joints. *J Compos Mater* 53(18):2607–2621. <https://doi.org/10.1177/0021998319836022>
 8. Sj A, Natarajan A (2022) Review on the advancements and relevance of emerging joining techniques for aluminum to polymers/carbon fiber-reinforced polymer lightweight hybrid structures. *Proc Inst Mech Eng Part L J Mater Des Appl* 236(12):2394–2435. <https://doi.org/10.1177/14644207221090331>
 9. Yalcinyüz A, Brunner-Schwer C, Biegler M, Rethmeier M (2023) Feasibility study of joining of carbon fiber-reinforced polymer composites and aluminum alloys by electron beam welding for use in lightweight construction. Presented at the 1st international conference on lightweight materials. Politecnico di Milano, Milan, Italy, p 68–73
 10. Węglowski B, Łach Phillips M (2016) Electron beam welding—techniques and trends—review. *Vacuum* 130:72–92. <https://doi.org/10.1016/j.vacuum.2016.05.004>
 11. Katayama S, Kawahito Y (2008) Laser direct joining of metal and plastic. *Scripta Mater* 59(12):1247–1250. <https://doi.org/10.1016/j.scriptamat.2008.08.026>
 12. Jung K-W, Kawahito Y, Takahashi M, Katayama S (2013) Laser direct joining of carbon fiber reinforced plastic to aluminum alloy. *J Laser Appl* 25(3):032003. <https://doi.org/10.2351/1.4794297>
 13. Engelmann C, Oster L, Olowinsky A, Gillner A, Mamuschkin V, Arntz D (2017) Novel process for butt-joined plastic-metal hybrid compounds. *J Laser Appl* 29(2):022416. <https://doi.org/10.2351/1.4983516>
 14. Georgiev DG, Baird RJ, Newaz G, Auner G, Witte R, Herfurth H (2004) An XPS study of laser-fabricated polyimide/titanium interfaces. *Appl Surf Sci* 236(1–4):71–76. <https://doi.org/10.1016/j.apsusc.2004.03.261>
 15. Tuna B, Benkreira H (2018) Chain extension of recycled PA6. *Polymer Eng Sci* 58(7):1037–1042. <https://doi.org/10.1002/polb.24663>
 16. Lamberti C, Solchenbach T, Plapper P, Possart W (2014) Laser assisted joining of hybrid polyamide-aluminum structures. *Phys Procedia* 56:845–853. <https://doi.org/10.1016/j.phpro.2014.08.103>
 17. RenAM 500 series material data sheet (2024) Renishaw plc. Available: <https://www.renishaw.com/resourcecentre/download?data=138868&lang=en&userLanguage=en>. Accessed 22 Apr 2025
 18. Vasiljević J et al (2020) Characterization of polyamide 6/ multilayer graphene nanoplatelet composite textile filaments obtained via in situ polymerization and melt spinning. *Polymers* 12(8):1787. <https://doi.org/10.3390/polym12081787>
 19. García-Zapata JM, Torres B, Rams J (2024) Effects of building direction, process parameters and border scanning on the mechanical properties of laser powder bed fusion AlSi10Mg. *Materials* 17(15):3655. <https://doi.org/10.3390/ma17153655>
 20. Lambiasi F, Yanala PB, Leone C, Paoletti A (2023) Repairing aluminum-PEEK hybrid metal–polymer joints made by thermomechanical joining. *J Manuf Process* 93:1–14. <https://doi.org/10.1016/j.jmapro.2023.03.018>
 21. Genna S, Moretti P, Ponticelli GS, Venettacci S (2024) Laser-based thermomechanical joining of semi-transparent thermoplastics with technical steel. *Int J Adv Manuf Technol* 132(7–8):3735–3755. <https://doi.org/10.1007/s00170-024-13624-6>
 22. Wang H, Ren Z, Guan Y (2022) Laser joining of continuous carbon fiber-reinforced PEEK and titanium alloy with high strength. *Polymers* 14(21):4676. <https://doi.org/10.3390/polym14214676>
 23. Klotzbach A, Langer M, Pautzsch R, Standfuß J, Beyer E (2017) Thermal direct joining of metal to fiber reinforced thermoplastic components. *J Laser Appl* 29(2):022421. <https://doi.org/10.2351/1.4983243>
 24. Feistauer EE, Guimarães RPM, Ebel T, dos Santos JF, Amancio-Filho ST (2016) Ultrasonic joining: a novel direct-assembly technique for metalcomposite hybrid structures. *Mater Lett* 170(1):1–4. <https://doi.org/10.1016/j.matlet.2016.01.137>
 25. Schrick K, Samfaß L, Grätzel M, Ecke G, Bergmann JP (2020) Bonding mechanisms in laser-assisted joining of metal–polymer composites. *J Adv Join Process* 1:100008. <https://doi.org/10.1016/j.jajp.2020.100008>

Publisher's Note Springer Nature remains neutral with regard to jurisdictional claims in published maps and institutional affiliations.